Chemical Science

ROYAL SOCIETY OF CHEMISTRY

EDGE ARTICLE

View Article Online
View Journal | View Issue

Open Access Article. Published on 14 September 2022. Downloaded on 3/12/2026 4:28:09 PM.
This article is licensed under a Creative Commons Attribution-NonCommercial 3.0 Unported Licence.

Check for updates

Cite this: *Chem. Sci.*, 2022, **13**, 12158

All publication charges for this article have been paid for by the Royal Society of Chemistry

Received 26th May 2022
Accepted 13th September 2022

DOI: 10.1039/d2sc02953g

rsc.li/chemical-science

Radical generation enabled by photoinduced N–O bond fragmentation†

Edward J. McClain, Alan K. Wortman and Corey R. J. Stephenson *

Recent advances in synthetic chemistry have seen a resurgence in the development of methods for visible light-mediated radical generation. Herein, we report the development of a photoactive ester based on a quinoline *N*-oxide core structure, that provides a strong oxidant in its excited state. The heteroaromatic *N*-oxide provides access to primary, secondary, and tertiary radical intermediates, and its application toward the development of a photochemical Minisci alkylation is reported.

Photoinduced radical generation has become a focal point of contemporary chemical research. Historically, the photochemical formation of radicals has been achieved *via* the direct irradiation of organic chromophores with high energy UV light, with notable examples including Norrish – type 1 reactions and the photochemical decomposition of azo compounds, peroxides, *N*-(acyloxy)-pyridones, and xanthates.[1] While a powerful tool, the propensity of organic functional groups to absorb UV light leads to undesired excitation events that ultimately result in uncontrolled, deleterious reactivity.[2] The use of visible light irradiation to drive reactivity offers a solution to the problems presented by UV light photochemistry, as typical organic functionalities do not absorb in the visible region of the electromagnetic spectrum. In this regard, photoredox catalysis has emerged as a powerful tool for the generation of radical intermediates, as the visible light absorbing catalysts can access high energy excited states that engage organic substrates in redox events.[3] While incredibly versatile, the manipulation of substrate oxidation states can limit the scope of reactivity, as functionalities that are predisposed to oxidation (or reduction) may undergo undesired side reactions. To circumvent this limitation, redox auxiliaries are employed to alter the redox properties of the substrate and facilitate reactivity under mild reducing (or oxidizing) conditions.[4]

Radical formation *via* photoinduced dissociation of an auxiliary, or complex, represents a complementary strategy that, in principle, should be tolerant of redox sensitive functionalities. However, despite the ubiquity of this strategy in UV light mediated reaction manifolds, the development of reagents that undergo efficient photodissociation upon visible light irradiation is limited. In 2017, Melchiorre and coworkers reported the dissociation of 4-alkyl-1,4-dihydropyridines (alkyl-DHPs) upon irradiation with 405 nm light (Fig. 1A).[5] Study of the photoactive

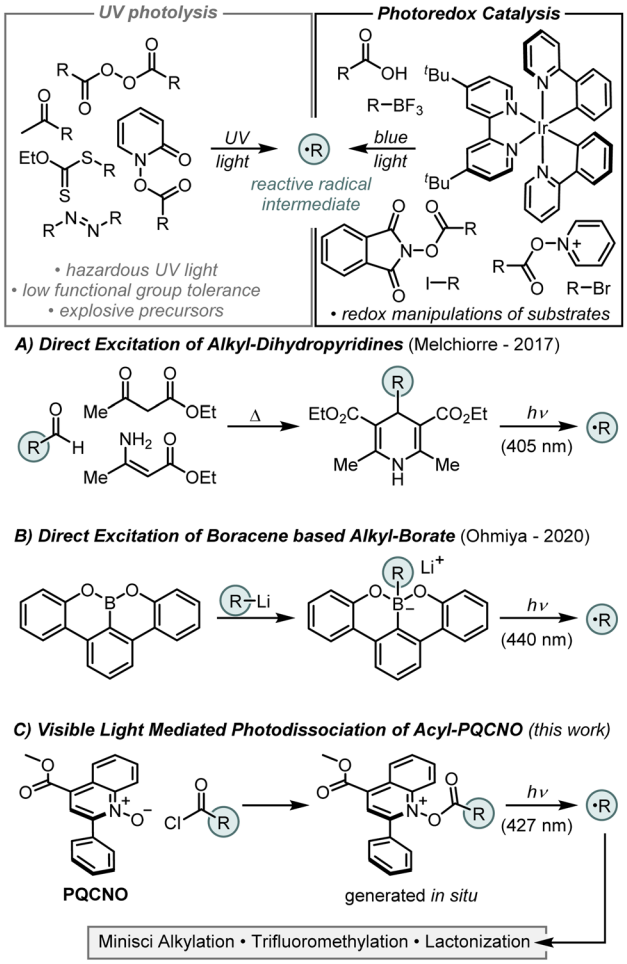

Fig. 1 Overview of photochemical radical generation in synthetic chemistry.

Willard Henry Dow Laboratory, Department of Chemistry, University of Michigan, 930 North University Avenue, Ann Arbor, Michigan 48109, USA. E-mail: crjsteph@umich.edu

† Electronic supplementary information (ESI) available: Experimental procedures, compound characterization, *in situ* LED NMR reaction procedure, UV-vis experiments, and fluorescence spectra. See https://doi.org/10.1039/d2sc02953g

© 2022 The Author(s). Published by the Royal Society of Chemistry

Open Access Article. Published on 14 September 2022. Downloaded on 3/12/2026 4:28:09 PM.
This article is licensed under a Creative Commons Attribution-NonCommercial 3.0 Unported Licence.

alkyl-DHPs revealed that they are reductants in their excited state ($D^{+\bullet}/D^* = -2.0$ V *vs.* SCE) and, as such, both the dissociative and redox properties of the excited state could be exploited for *ipso*-substitution of aryl nitriles and nickel catalyzed C(sp^2)–C(sp^3) cross-coupling reactions.

In 2020, Ohmiya and colleagues reported that boracene, when reacted with organolithium or Grignard reagents, forms a photoactive alkyl borate salt that liberates an equivalent of an alkyl radical upon irradiation with 440 nm light (Fig. 1B).[6] Characterization of the boracene-based alkyl borate revealed a strongly reducing excited state ($B^{+\bullet}/B^* = -2.2$ V *vs.* SCE), and this auxiliary was demonstrated to be effective for nickel catalyzed C(sp^2)–C(sp^3) cross-coupling reactions with tertiary alkyl radicals.

Pioneering work by Barton and coworkers in the 1980's demonstrated that the thermal or photochemical decomposition of *N*-(acyloxy)-2-thiopyridones (commonly referred to as Barton esters) could efficiently generate carbon centered radicals, ultimately delivering the corresponding alkane or thioether products.[7] However, state-of-the-art methods employing pyridine *N*-oxide or its derivatives as radical precursors have demonstrated limited intermolecular reactivity, as the generated radical intermediates are competitively trapped by the pyridine-based auxiliary.[8,9] To overcome these limitations, we sought to design a pyridine *N*-oxide based auxiliary that does not undergo undesired alkylation reactions. Inspired by Barton's work and informed by our previous studies,[8,9] we envisioned that the fast fragmentation of N–O bonds in pyridine *N*-oxide derivatives could be leveraged in the design of a photocleavable activator that would deliver carbon centered radicals from readily available carboxylic acids as precursors. Importantly, the development of a photoactive ester derived from simple pyridine *N*-oxide core structure delivers a species that is a strong oxidant in its excited state, complementing the reductive excited states of the previously developed photoactive auxiliaries. Moreover, by using a core structure that is derived from an abundant heteroaromatic building block, the designed photoactive esters will contain highly tunable core structures, allowing for control over the photoexcitation and fragmentation events. Herein, we report the development of a photoactive ester derived from a quinoline *N*-oxide core structure and its application to achieve an efficient intermolecular Minisci alkylation (Fig. 1C).

At the outset of our study, we established several requirements to be satisfied by potential photoactive esters (Fig. 2B): (1) the pyridine *N*-oxide core structure needed to be preserved, (2) the heteroaromatic core would need to have blocking substituents at the sites of alkylation to slow deleterious functionalization of the ester (*i.e.* 2-, 4-, and 6-substituted pyridine *N*-oxide derivatives), (3) the heteroaromatic *N*-oxide would need to maintain sufficient nucleophilicity to form the activated *N*-acyloxy pyridinium, (4) the heteroaromatic backbone would need to deliver a sterically accessible *N*-oxide functionality. Additionally, it was recognized that pyridine *N*-oxide derivatives bearing alkyl substituents with benzylic C–H bonds were not suitable photoactive esters, as a deleterious Boekelheide reaction occurred upon acylation of the *N*-oxide functionality.

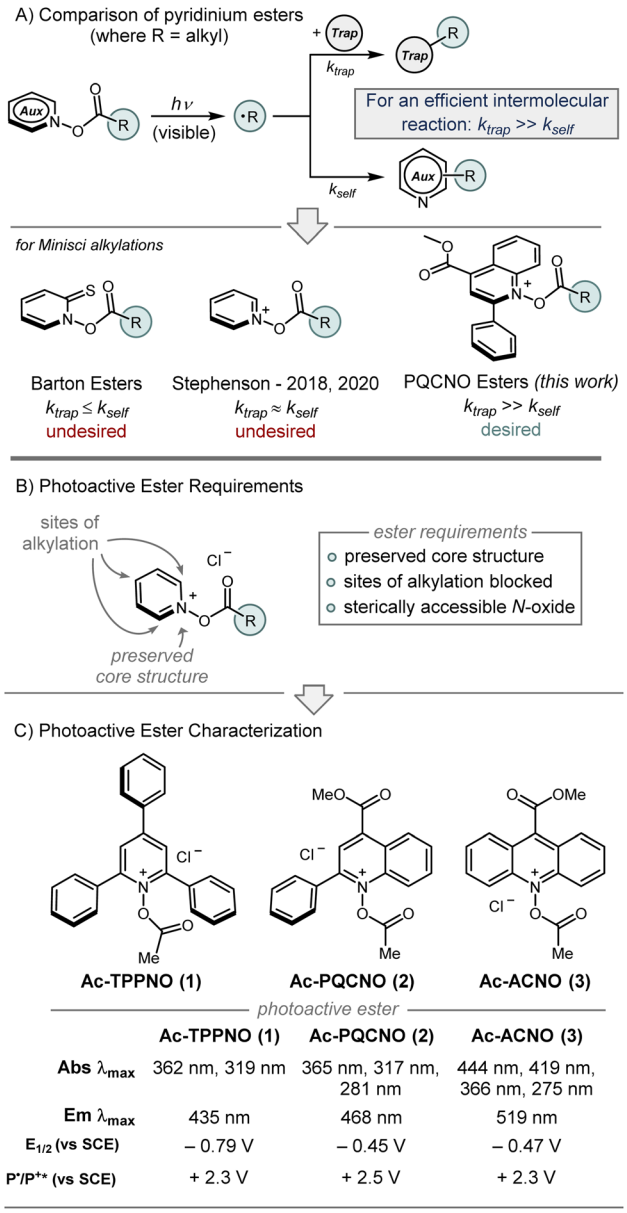

Fig. 2 (A) Comparison of pyridinium esters. (B) Overview of photoactive ester design principles. (C) Photophysical characterization of Ac-TPPNO, Ac-PQCNO, and Ac-ACNO.

Ultimately, 2,4,6-triphenyl pyridine *N*-oxide (TPPNO), methyl 2-phenylquinoline-4-carboxylate *N*-oxide (PQCNO), and methyl acridine-9-carboxylate *N*-oxide (ACNO) were identified as potential photoactive ester precursors that met all aforementioned requirements.

Initial investigations focused on the photophysical characterization of the three heteroaromatic *N*-oxides (Fig. 2C). Uv-vis spectroscopy in acetonitrile revealed TPPNO to have two maximum absorbances at 319 nm and 365 nm, with the latter absorbance tailing off beyond 400 nm. PQCNO and ACNO also displayed a strong absorbance feature at 365 nm, however, for ACNO two additional lower energy absorbance features at 418 nm and 444 nm were observed. Addition of acetyl chloride

Open Access Article. Published on 14 September 2022. Downloaded on 3/12/2026 4:28:09 PM.
This article is licensed under a Creative Commons Attribution-NonCommercial 3.0 Unported Licence.

to TPPNO and PQCNO resulted in an increase of intensity for the absorbance features, with no apparent shift in the absorbance maxima. Acylation of the ACNO auxiliary with acetyl chloride caused the maximum at 274 nm to diverge into two distinct sharp absorbance features with maxima at 264 nm and 275 nm. Additionally, the absorbance feature at 364 nm both increased in intensity and became more structured upon acylation, revealing an apparent shoulder at 352 nm. Measurement of the fluorescence spectra for the heteroaromatic *N*-oxides (irradiated at 361 nm) revealed that Ac-TPPNO, Ac-PQCNO, and Ac-ACNO have emission maxima at 435 nm, 468 nm and 519 nm, respectively (Fig. 3A). In the absence of an acyl equivalent, no emission was observed for the heteroaromatic *N*-oxides. This finding is consistent with previous reports that pyridine *N*-oxides and quinoline *N*-oxides possess non-emissive excited states under basic conditions due to a propensity to undergo a fast rearrangement on the singlet surface.[10]

Investigation of the photoinduced N–O bond cleavage of Ac-PQCNO revealed that upon successive fluorescence scans (excitation at 335 nm), Ac-PQCNO is observed to decompose steadily with the concomitant appearance of the fluorescence signal corresponding to the generation of deoxygenated quinoline (Fig. 3B). Interrogation of the decomposition by Uv-vis spectroscopy revealed that after 60 s of irradiation of Ac-PQCNO with a 427 nm Kessil lamp, a decrease in the absorbance feature at 365 nm was observed. Upon extending irradiation time out to 30 min, significant degradation of the Ac-PQCNO was observed.

Together, the photophysical characterization shows the photoactive esters possess conserved absorption features at 365 nm. Consistent with previous studies on quinoline *N*-oxide photochemistry, the absorption feature at 365 nm is thought to be π,π* in character and responsible for the observed deoxygenation reactivity.[11] The deoxygenation of the aromatic *N*-oxides is hypothesized to arise from crossing over of the π,π* excited state to a dissociative π,σ* state. Computational evidence in support of the hypothesized mechanism can be found in Fukuda and Ehara's study on the deoxygenation of structurally related *N*-hydroxypyridine-2(1*H*)-thione.[12] Experimental support for this proposed mechanism can be found in Hata and Tanaka's study of the gas phase photolysis of pyridine *N*-oxide[13] as well as Hata's subsequent translation of this work to the solution phase photodeoxygenation of heteroaromatic *N*-oxides in the presence of a strong Lewis acid, $BF_3 \cdot Et_2O$.[14]

Interrogation of the thermal reactivity of Ac-PQCNO revealed there was no deoxygenation of the heteroaromatic *N*-oxide after heating to 90 °C for 3 hours. This demonstrates that the remarkable reactivity of Ac-PQCNO is due to dissociation of the N–O bond from a low energy photoexcited state.

Electrochemical analysis of the heteroaromatic *N*-oxide photoactive esters using cyclic voltammetry in acetonitrile revealed the Ac-TPPNO, Ac-PQCNO, and Ac-ACNO to have low energy reduction waves, with measured $E_{1/2}$ of −0.79 V *vs.* SCE, − 0.45 V *vs.* SCE, and −0.47 V *vs.* SCE. Applying information gathered from absorbance and emission spectroscopy, as well as the electrochemical data, the standard potential for oxidation of Ac-TPPNO, Ac-PQCNO and Ac-ACNO in the excited state was estimated to be +2.30 V [$E^0(T^{+*}/T^{\bullet})$], +2.57 V [$E^0(P^{+*}/P^{\bullet})$], and +2.32 V [$E^0(A^{+*}/A^{\bullet})$] *vs.* SCE according to the Rehm–Weller approximation (Fig. 2C).[15]

Due to the mild photolytic conditions for decarboxylative radical generation from *N*-oxides and characteristics as excited state oxidants, we sought to assess the reactivity of the photocleavable esters towards the development of an intermolecular Minisci alkylation (Fig. 4). Initial studies focused on the addition of the *tert*-butyl radical to 4-chloroquinoline in acetonitrile.

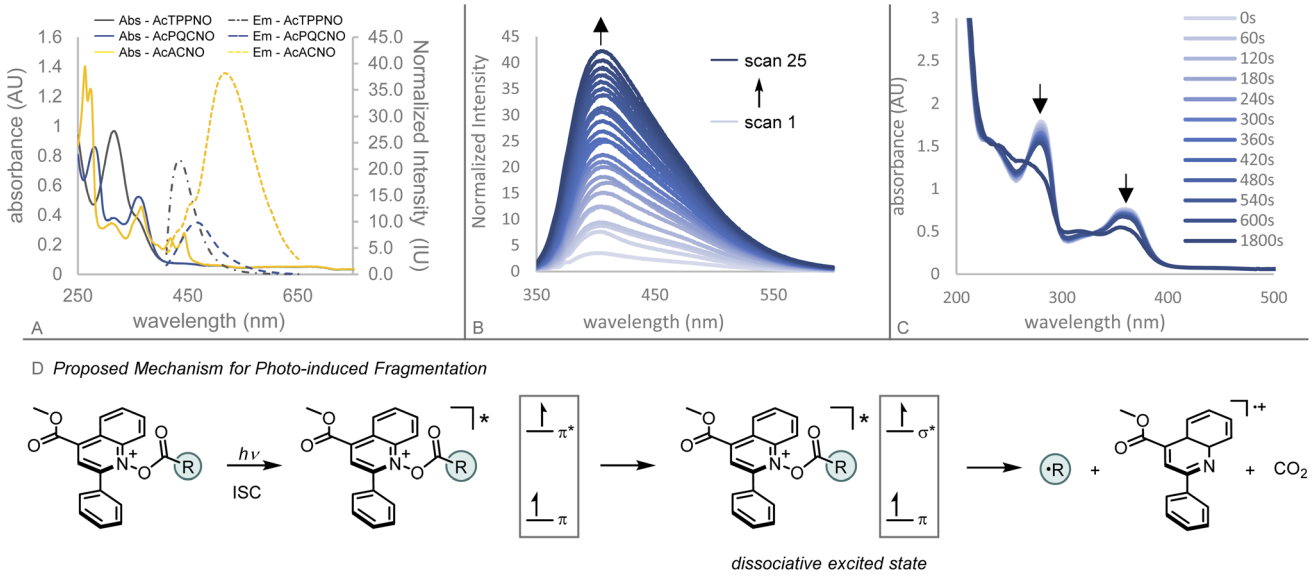

Fig. 3 (A) Absorbance and emission spectra for Ac-TPPNO, Ac-PQCNO, and Ac-ACNO. Emission recorded upon irradiation at 361 nm. (B) Fluorescence spectra of Ac-PQCNO monitored over 25 successive scans (excitation 335 nm). (C) Decomposition of Ac-PQCNO upon irradiation by a 427 nm Kessil lamp, monitored by Uv-vis. (D) Proposed mechanism for photochemical decomposition of Ac-PQCNO.

 © 2022 The Author(s). Published by the Royal Society of Chemistry

Open Access Article. Published on 14 September 2022. Downloaded on 3/12/2026 4:28:09 PM.
This article is licensed under a Creative Commons Attribution-NonCommercial 3.0 Unported Licence.

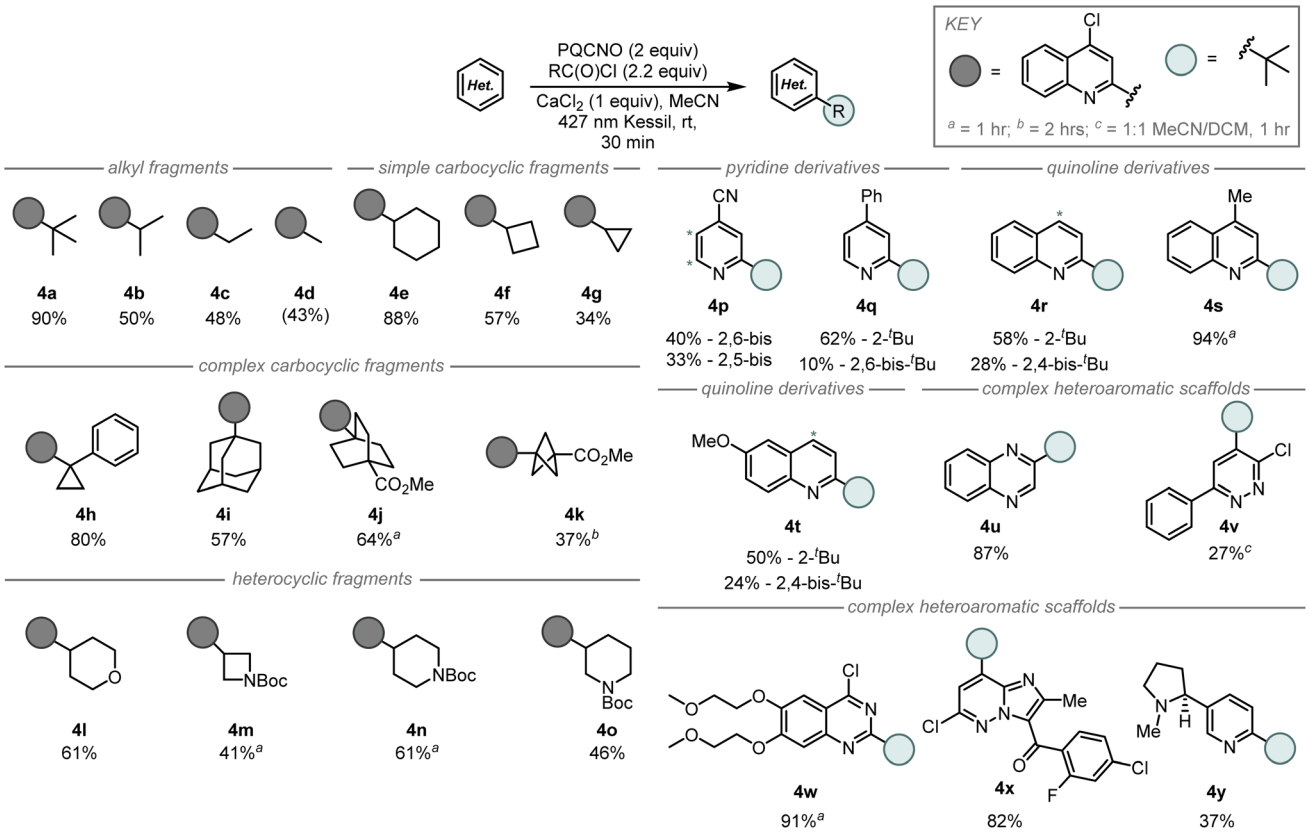

Fig. 4 Scope of intermolecular Minisci alkylation. Isolated yields unless otherwise noted. Standard conditions: substrate (0.2 mmol, 1 equiv.), PQCNO (2 equiv.), acyl chloride (2.2 equiv.), $CaCl_2$ (1 equiv.), MeCN (0.5 mL), N_2 atmosphere, 427 nm Kessil lamp, 30 min. [a]Reaction run for 1 hour. [b]Reaction run for 2 hours. [c]Reaction run for 1 hour with a 1 : 1 mixture of MeCN to DCM as solvent. NMR yield with methyl *tert*-butyl ether as internal standard, in brackets.

Assessment of reactivity revealed TPPNO and PQCNO to perform identically under unoptimized conditions delivering 27% of the desired 2-*tert*-butyl-4-chloroquinoline product, while ACNO produced less than 5% of the desired product. Due to the low cost of the parent quinoline and its high yielding N-oxidation,[16] we elected to focus our investigations on the application of PQCNO as a photoactive ester. Degassing the reaction resulted in a substantial increase in yield, providing 90% isolated yield of the desired product. Further investigation of solvents and additives did not result in increased reactivity.

Assessment of the scope for the intermolecular Minisci alkylation revealed the *tert*-butyl radical addition was the most efficient of the simple alkyl fragments (90%, **4a**), followed by isopropyl addition (50%, **4b**), ethyl addition (48%, **4c**), and finally methyl addition (43%, **4d**) (Fig. 4). Simple carbocyclic radical fragments such as cyclohexyl (**4e**), cyclobutyl (**4f**), and cyclopropyl (**4g**) provided the corresponding alkylation products in 88%, 57%, and 34% yield, respectively. Interestingly, Minisci alkylation products from more complex carbocyclic radical fragments were also accessible under-developed reaction conditions as 1-phenylcyclopropyl (**4h**), adamantyl (**4i**), 4-(methoxycarbonyl)-[2.2.2]-bicycloctyl (**4j**), and 3-(methoxycarbonyl)-[1.1.1]-bicyclopentyl (**4k**) fragments gave the corresponding radical addition products in 37–80% yield. Application of tetrahydropyran-4-carbonyl chloride (**4l**), *N*-Boc azetidine 3-carbonyl chloride (**4m**), *N*-Boc piperidine 4-carbonyl chloride (**4n**), and *N*-Boc piperidine 3-carbonyl chloride (**4o**) provided the desired coupling products in 41–61% yield, respectively.

Assessment of the heterocyclic coupling partners revealed that substituted pyridine and quinoline derivatives performed well in the Minisci alkylation, however, over-alkylation of the heteroarene was often observed (**4p–4t**). Notably, 4-cyanopyridine (**4p**) and lepidine (**4s**) performed well under the developed intermolecular reaction conditions; these substrates were either low yielding or inaccessible under our previously reported fragment coupling conditions.[8] Modestly complex heteroaromatic scaffolds such as quinoxaline (**4u**), and 3-chloro-6-phenylpyridazine (**4v**) also performed well under the *tert*-butylation reaciton conditions. Biologically active scaffolds such as the 4-chloroquinazoline core of erlotinib (**4w**) and the imidazopyrazine core structure of gandotinib (**4x**) each provided a single regioisomer of the *tert*-butyl addition product in high yield. Finally, nicotine (**4y**) was observed to undergo *tert*-butyl addition in 37% yield with retention of the configuration at the benzylic stereocenter.

During the exploration of the Minisci alkylation reaction, it was realized that the deoxygenated quinoline could be

Open Access Article. Published on 14 September 2022. Downloaded on 3/12/2026 4:28:09 PM.
This article is licensed under a Creative Commons Attribution-NonCommercial 3.0 Unported Licence.

recovered in high yields (87% recovery). Resubjecting the recovered quinoline to oxidation conditions, PQCNO could be re-generated in 71% yield. Regenerated PQCNO was observed to show no decrease in reactivity when recycled through three consecutive reactions (see ESI†).

To probe the mechanism of the photoinduced Minisci alkylation reaction, we monitored the reaction by employing an *in situ* LED NMR device equipped with a 430 nm LED source. Investigation of the N–O bond fragmentation revealed that the rate of deoxygenation was not dependent on the rate of decarboxylation for the acyloxy group. Benzoyloxy and pivaloyloxy substituted *N*-oxides provided similar rates of deoxygenation ($k_{obs} = -5.8 \times 10^{-5}$ M s^{-1} (BzO–) *vs.* $k_{obs} = -6.3 \times 10^{-5}$ M s^{-1} (PivO–); see ESI†), a result that is interesting given the difference in rates of decarboxylation form the respective carboxylic acids.[17,18] Alteration of the aryl substituent in the 2-position of the PQCNO auxiliary was observed to impact the rate of deoxygenation, as *ortho* substituted 2,6-dimethylphenyl substituent provided an increased rate of deoxygenation ($k_{obs} = -7.9 \times 10^{-5}$ M s^{-1}), whereas electron rich *para*-methoxyphenyl substituent led to a substantial decrease in the observed rate for deoxygenation ($k_{obs} = -2.2 \times 10^{-5}$ M s^{-1}).

Monitoring the deoxygenation of Piv-PQCNO under reaction conditions revealed an increase in the observed rate of deoxygenation in the presence of 4-chloroquinoline (Fig. 5A). We hypothesize that the change in rate for deoxygenation is indicative of a propagative reaction mechanism in which electron transfer from the radical addition product (**III**) to acylated PQCNO (**I**) leads to formation of the final C–H alkylated product as well as generating a second equivalent of R$^{\bullet}$ through a reductive decarboxylation of acylated PQCNO (I). Determination of the quantum yield (Φ) for the decomposition of Piv-PQCNO supported the proposed propagative chain mechanism, in the presence of 4-chloroquinoling $\Phi = 0.983$ whereas in the absence of a substrate $\Phi = 0.218$ for Piv-PQCNO decomposition. The increase in observed quantum yield is indicative of chain mechanism promoting Piv-PQCNO decomposition in the presence of a substrate. Further support was found when subjecting 2-phenylpropionyl chloride to the reaction conditions in the absence of a heteroaromatic substrate, 1-chloro-1-phenylethane was observed (see ESI†), demonstrating the ability of acyl PQCNO to oxidize stabilized radical intermediates.

On the basis of these findings, we propose the following mechanism (Fig. 5B). Initiation of the Minisci alkylation occurs by the photoinduced decomposition of acyl-PQCNO (**I**) to generate an equivalent of a reactive radical intermediate (R$^{\bullet}$). Addition of R$^{\bullet}$ to an equivalent of the protonated heteroaromatic substrate provides intermediate (**II**). Deprotonation of (**II**) generates radical intermediate (**III**) that is in turn oxidized by a second equivalent of acyl-PQCNO (**I**), providing the desired C–H alkylated product while generating a second equivalent of R$^{\bullet}$ through the decomposition of reduced acyl-PQCNO (**IV**), thereby propagating the reaction.

Finally, we sought to explore alternate radical transformations that can be promoted by PQCNO-based esters (Scheme 1). Lactonization of 2-phenylbenzoyl chloride was carried out, providing moderate yield for the 3,4-benzocoumarin product.[20] By employing trifluoroacetic anhydride (TFAA) as an acyl equivalent in the presence of *tert*-butyl anisole, radical trifluoromethylation of the electron-rich arene was achieved in

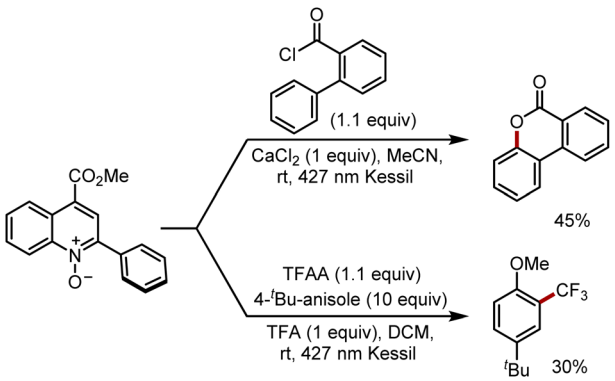

Scheme 1 Alternate radical transformations.

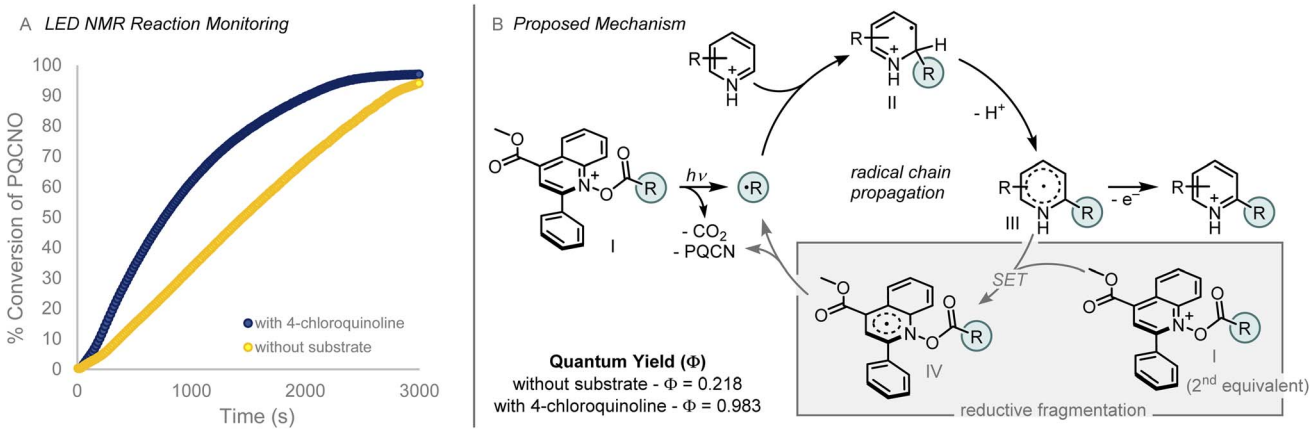

Fig. 5 (A) Reaction profile in the presence (blue) and absence (yellow) of substrate, monitored using 430 nm LED NMR apparatus. (B) Proposed mechanism for photomediated Minisci reaction.[19]

 © 2022 The Author(s). Published by the Royal Society of Chemistry

Open Access Article. Published on 14 September 2022. Downloaded on 3/12/2026 4:28:09 PM.
This article is licensed under a Creative Commons Attribution-NonCommercial 3.0 Unported Licence.

moderate yields.[8] Further assessments of reactivity are currently ongoing within our laboratory.

In conclusion, we have developed a photoactive ester based upon the quinoline *N*-oxide core which delivers a strong oxidant in its excited state. The designed photocleavable ester enabled the development of a photochemical Minisci alkylation, providing a reaction platform that leveraged both the photochemical dissociation and the oxidizing characteristics of the photoactive esters. The photochemical reactivity of the PQCNO ester was also demonstrated to effect radical lactonization and trifluoromethylation reactions.

Abbreviations

TPPNO	Triphenylpyridine *N*-oxide
PQCNO	Methyl 2-phenylquinoline-4-carboxylate *N*-oxide
PQCN	Methyl 2-phenylquinoline-4-carboxylate
ACNO	Methyl acridine-9-carboxylate *N*-oxide

Data availability

The data supporting this article are available in the manuscript and in the ESI.†

Author contributions

The manuscript was written through contributions of all authors. All authors have given approval to the final version of the manuscript.

Conflicts of interest

The authors have no conflicts of interest to declare.

Acknowledgements

The financial support was provided by the National Science Foundation Division of Chemistry (CHE-1900266) and the University of Michigan. We would like to thank Nathaniel Szymczak for allowing us to use his group's Uv-vis spectrophotometer.

References

1 (*a*) M. Oelgemöller and N. Hoffman, *Org. Biomol. Chem.*, 2016, **14**, 7392; (*b*) N. A. Porter and L. J. Marnett, *J. Am. Chem. Soc.*, 1973, **95**, 4361; (*c*) M. D. Spantulescu, R. P. Jain, D. J. Derksen and J. C. Vederas, *Org. Lett.*, 2003, **5**, 2963; (*d*) E. C. Taylor, H. W. Altland, F. Kienzle and A. McKillop, *J. Org. Chem.*, 1976, **41**, 24; (*e*) S. Z. Zard, *Angew. Chem., Int. Ed.*, 1997, **36**, 672.
2 M. D. Kärkäs, J. A. Porco and C. R. J. Stephenson, *Chem. Rev.*, 2016, **116**, 9683.
3 (*a*) M. H. Shaw, J. Twilton and D. W. C. MacMillan, *J. Org. Chem.*, 2016, **81**, 6896; (*b*) R. C. McAtee, E. J. McClain and C. R. J. Stephenson, *Trends Chem.*, 2019, **1**, 111.
4 (*a*) K. Okada, K. Okamoto, N. Morita, K. Okubo and M. Oda, *J. Am. Chem. Soc.*, 1991, **113**, 9401; (*b*) J. W. Beatty, J. J. Douglas, K. P. Cole and C. R. J. Stephenson, *Nat. Commun.*, 2015, **6**, 7919; (*c*) J. K. Matsui, D. N. Primer and G. A. Molander, *Chem. Sci.*, 2017, **8**, 3512.
5 L. Buzzetti, A. Prieto, S. R. Roy and P. Melchiorre, *Angew. Chem., Int. Ed.*, 2017, **56**, 15039.
6 (*a*) Y. Sato, K. Nakamura, Y. Sumida, D. Hashizume, T. Hosoya and H. Ohmiya, *J. Am. Chem. Soc.*, 2020, **142**, 9938; (*b*) Y. Miyamota, Y. Sumida and H. Ohmiya, *Org. Lett.*, 2021, **23**, 5865.
7 (*a*) D. H. R. Barton, D. Crich and W. B. Motherwell, *Tetrahedron Lett.*, 1983, **24**, 4979; (*b*) D. H. R. Barton, B. Lacher and S. Zard, *Tetrahedron*, 1987, **43**, 4321. For a review, see: (*c*) M. F. Saraiva, M. R. C. Couri, M. Le Hyaric and M. V. de Almeida, *Tetrahedron*, 2009, **65**, 3563.
8 A. C. Sun, E. J. McClain, J. W. Beatty and C. R. J. Stephenson, *Org. Lett.*, 2018, **20**, 3487.
9 E. J. McClain, T. M. Monos, M. Mori, J. W. Beatty and C. R. J. Stephenson, *ACS Catal.*, 2020, **10**, 12636.
10 (*a*) A. Alkaitis and M. Calvin, *Chem. Commun.*, 1968, 292; (*b*) N. Hata and I. Ono, *Bull. Chem. Soc. Jpn.*, 1975, **49**, 1794; (*c*) C. Kaneko, H. Fuji, S. Kawai, K. Hashiba, Y. Karasawa, M. Wakai, R. Hayashi and M. Somie, *Chem. Pharm. Bull.*, 1982, **30**, 74.
11 (*a*) P. L. Kulmer and O. Buchardt, *Chem. Commun.*, 1968, 1321; (*b*) K. Tokumura and Y. Matsushita, *J. Photochem. Photobiol., A*, 2001, **140**, 27; (*c*) G. G. Aloisi and G. Favaro, *J. Chem. Soc., Perkin Trans. 2*, 1976, 456; (*d*) For review of *N*-oxide photochemistry, see: A. Albini and M. Alpegiani, *Chem. Rev.*, 1984, **84**, 43.
12 R. Fukuda and M. Ehara, *Theor. Chem. Acc.*, 2016, **135**, 105.
13 N. Hata and I. Tanaka, *J. Chem. Phys.*, 1962, **36**, 2072.
14 H. Norisuke, O. Isao and K. Masao, *Chem. Lett.*, 1975, **4**, 25.
15 D. Rehm and A. Weller, *Isr. J. Chem.*, 1970, **8**, 259.
16 2,4,6-Triphenyl pyridine is unreactive towards N-oxidation and, thus, the by product goes to waste. Methyl 2-phenylquinoline-4-carboxylate can be recovered and recycled in high yields.
17 J. Catheauneuf, J. Lusztky and K. U. Ingold, *J. Am. Chem. Soc.*, 1988, **110**, 2886.
18 J. W. Hilborn and J. A. Pincock, *J. Am. Chem. Soc.*, 1991, **113**, 2683.
19 It is believed that a small amount of HCl is generated from the reaction of adventitious water in the system reacting with $CaCl_2$ or the acyl chloride. The remaining acid in the system is believed to arise as a by product of the reaction.
20 N. P. Ramirez, I. Bosque and J. C. Gonzalez-Gomez, *Org. Lett.*, 2015, **17**, 4550.